Hopping transport on a fractal: ac conductivity of porous silicon

M. Ben-Chorin, F. Möller, and F. Koch
Physik-Department E16, Technische Universität München, D-85747 Garching, Germany

W. Schirmacher and M. Eberhard
Physik-Department E13, Technische Universität München, D-85747 Garching, Germany
(Received 17 June 1994; revised manuscript received 2 September 1994)

We have measured the frequency dependence of the conductivity and the dielectric constant of various samples of porous Si in the regime 1 Hz–100 kHz at different temperatures. The conductivity data exhibit a strong frequency dependence. When normalized to the dc conductivity, our data obey a universal scaling law, with a well-defined crossover in which the real part of the conductivity σ' changes from an $\omega^{1/2}$ dependence to being proportional to ω. We explain this in terms of activated hopping in a fractal network. The low-frequency regime is governed by the fractal properties of porous Si, whereas the high-frequency dispersion comes from a broad distribution of activation energies. Calculations using the effective-medium approximation for activated hopping on a percolating lattice give fair agreement with the data.

I. INTRODUCTION

The discovery of efficient luminescence from porous Si (PS) (Refs. 1 and 2) has created a great deal of interest in this material, because of its possible applications in Si-based optoelectronics. Porous Si is produced by electrochemical etching of crystalline, doped Si in a hydrofluoric acid (HF) electrolyte. The resulting material is an interconnected network of small Si crystallites with a typical size of a few tens of Å.[3] Porous Si has quite efficient photoluminescence in the visible range, above the band gap of crystalline Si. The effect has been linked to quantum confinement of carriers inside the small crystallites, which results in an increased band gap.[1,4] A lot of research is currently devoted to the optical properties of this material. Very little, however, is known regarding its electrical transport properties.

While quantum confinement is necessary to explain the luminescence properties of PS, it is not clear whether the same is true for the transport properties. Porous Si is insulating, with a typical resistivity at room temperature that is five orders of magnitude higher than that of intrinsic Si.[5–7] This high resistivity can be attributed to various effects. Assuming that the material can be regarded as a semiconductor, quantum confinement results in a wider band gap and reduces the thermal generation of free carriers. However, this requires that the carriers supplied by doping are depleted. Depletion of carriers is known to occur during the preparation of the material, either because the dopant energies are increased, or because of the creation of deep surface levels.[4]

However, the simple model of a wide band-gap semiconductor, where dopants are depleted resulting in intrinsic characteristics, does not apply for the transport. Different authors have measured the activation energy of the dc conductivity, and have reported values about 0.5 eV.[7,8] This energy is lower than half the "band gap," extracted from luminescence measurements, suggesting that the material is not "intrinsic." The value 0.5 eV is comparable to the activation energy in intrinsic crystalline Si. To explain the lower conductivity the effective mobility of carriers in PS should be much reduced by comparison with bulk Si. These arguments suggest that the mobility of carriers in PS is governed by a completely different process.

One feature that strongly affects the transport is the inhomogeneous nature of the material. The current is carried in regions with high local conductivity, which occupy only a small fraction of the material volume. From a comparison of electron microscopy data with computer models,[9] as well as from small-angle x-ray[10,11] and neutron[12] scattering, it is known that the PS network of crystallites has a fractal structure. Such a structure is expected to have strong geometrical effects on the conductivity.

Another important feature is disorder induced localization. Although PS preserves the crystalline structure on short length scales, and even long-range order in the sense of a common orientation of the crystallites is conserved to some degree, one must keep in mind that the material is highly irregular. Since the crystallites have different sizes and shapes, there are band-gap variations from one particle to another. These band-gap fluctuations are likely to cause localization of the electronic states. Like in an amorphous semiconductor, the system has a spectrum of localized energy levels that results from the disorder.

In such a system, transport can occur in various ways.[13,14] Carriers can be activated to a mobility edge above which extended states exist or to an energy above which they can move by hopping transport. In this case the activation energy of 0.5 eV, observed in the dc conductivity experiments, reflects the energy separation between the Fermi level and the mobility (or transport) edge. The conductivity would behave as in the wide

band-gap semiconductor picture, except for a reduced mobility relative to crystalline Si because of an enhanced scattering due to the disorder.

There exists also the possibility of hopping in the vicinity of the Fermi level.[13] This requires localized states within k_BT around the Fermi level. The dc activation energy is then a typical barrier height separating neighboring localized states.

There are two questions to be answered. The first is whether the high resistivity of PS has a physical origin such as quantum confinement, or is due to a geometrical effect. Second, the basic mechanism of transport in the material must be determined. These questions can be answered using combined dc and ac conductivity measurements, because the ac conductivity probes the local conductivity of the composite material.

ac conductivity measurements[15,16] have been extensively used to investigate both amorphous and glassy materials, as well as different ceramic and granular systems.[18] They allow one to investigate the broad range of relaxation times typical for nonhomogeneous and amorphous systems. In this way, it is possible to obtain more information on the underlying transport mechanism than from dc conductivity measurements alone.

Different approaches are used for the two classes of materials. For ceramics and granular composites classical effective-medium theories are applied.[19,20] The dispersion of the ac conductivity is given by a nontrivial average involving the ac conductivity of the crystallites (Si) and that of the matrix in which they are embedded (air). The averaging procedure accounts for the properties of the material and the geometry of the connecting network. This method has been used to interpret the IR properties of PS.[21] However, it completely neglects quantum effects like tunneling between particles, which is important for the conductivity. This will not affect the results in the IR regime, which is dominated by the intraparticle polarization. The low-frequency conductivity will have large contributions from tunneling processes. This is the case in amorphous and glassy materials, where the structure is homogeneous and the dispersion comes from the disorder.

Usually, hopping transport between localized states is the reason for the frequency dependence of the conductivity. The disorder results in a wide distribution of hopping rates, and gives a strong dispersion of the ac conductivity. In most of the systems investigated, a frequency dependence for the real part of the conductivity $\sigma'(\omega)$ of the form[13,15–17]

$$\sigma'(\omega) \propto \omega^v \tag{1}$$

(with $0 < v \leq 1$, but mostly $v \approx 1$) is observed. This frequency dependence usually relates a small dc conductivity to a high local one which (with increasing frequency) is due to the polarization of increasingly small conducting units.

The reduction of the dc conductivity is intimately related to the appearance of the frequency law (1). Although this behavior of the ac conductivity has been termed "universal"[15,22] because it is ubiquitous in disordered materials, it can have different microscopic origins.[23,24] For electronic transport, the relevant mechanisms are electron localization with associated hopping[25,13,14] and fractal topology.[26] In both cases, the experimental data can be represented in a scaling form,[27]

$$\sigma'(\omega) = \sigma'(0)\, f\left(\frac{\omega}{\sigma'(0)}\right). \tag{2}$$

The scaling function $f(x)$, which describes the crossover from the frequency-independent to the frequency-dependent regime, has a limiting behavior,

$$f(x) \propto \begin{cases} \text{const} & x \ll x_0 \\ x^v, & x \gg x_0 \end{cases}. \tag{3}$$

If the dc conductivity is temperature dependent, one can combine the dc and ac data to obtain a master plot which explores many orders of magnitude of the universal scaling function.

In this present study of the conductivity of PS, we indeed obtain a scaling behavior as indicated by Eq. (2). In contrast to other disordered systems, our scaling function exhibits *two crossovers*, namely,

$$f(x) \propto \begin{cases} \text{const}, & x \ll x_0 \\ x^u, & x_0 \ll x \ll x_1 \\ x^v, & x \gg x_1 \end{cases} \tag{4}$$

with $u \approx 0.5$ and $v \approx 1$. The lower frequency x_0 defines the crossover from dc conduction to a regime, where, as we argue, the frequency dependence is produced by the fractal geometry of PS. The higher one, x_1, is the crossover to hopping transport, with a wide distribution of local hopping conductances within a given crystallite or between near neighbors. We confirm this conjecture by a model calculation using the effective-medium approximation (EMA) for an activated hopping model on a percolating lattice.

II. EXPERIMENTAL ASPECTS

The porous samples are prepared by anodization of p-type Si in the dark. The substrate material is (100) Si, doped with B to a resistivity of 5 Ω cm. Before anodization, an Ohmic contact to the substrate is created, by evaporating a thin layer of Al, followed by annealing at 555 °C for 20 min. The current-voltage characteristic of this contact was checked and found to be linear. Anodization is done in a solution of HF (49% by wt.) diluted 1:1 by volume with ethanol. The etch current density is 30 mA/cm^2. Immediately after anodization the samples are taken out from the cell, rinsed with propanol, and left to dry in ambient conditions. For electrical measurements, rectangular aluminum contacts (2×1 mm^2) are evaporated on top of the porous layer. Samples prepared in the dark and without further chemical treatment, exhibit only weak luminescence at 1.7 eV. This is nonluminescing PS, in the usual sense.

The ac conductivity is measured by applying a sinu-

soidal voltage between the aluminum contact and the Ohmic back contact, and measuring the current after amplification using a lock-in technique. At each measuring frequency the lock-in phase is adjusted by replacing the sample with a 1 MΩ resistor. Then the current through the sample is measured in both the resistive and capacitive phases, and the results are calibrated with comparison to the resistor.

We need to comment on some experimental problems which affect the interpretation of the ac conductivity measurements. Transport in insulating materials is known to be nonlinear. This is the case in PS. The dc conductivity is in principle field dependent.[8] We have checked the ac current for different ac voltages in the range 0.1-10 V rms. Only a slight increase of the measured conductivity is observed (about 10%). As we shall see, this small change is negligible in comparison to the observed dispersion. Thus, we may assume that our measurements are in the linear regime. To minimize errors our measurements have been carried out with a fixed excitation voltage of 1 V. For the given sample this corresponds to about 10^{-3} V/cm.

Another problem is the question of contacts.[18] The measured admittance $Y = I/V$ is usually interpretated as a parallel combination of conductance and capacitance, $Y = G + i\omega C$, where G is related to the conductivity and C to the dielectric constant of the PS. Contact resistances and capacitance spoil this interpretation. We examine in Fig. 1 the dependence of the conductivity and the dielectric constant on frequency for two samples with different thicknesses. The dielectric constant does not depend significantly on the PS layer thickness. The conductivity is independent of thickness only for low frequencies. At high frequencies, one finds that the thicker sample has higher effective conductivity. This can be easily explained if one takes into account the contact resistance. An equivalent circuit for the measurement is given in the inset of Fig. 1. Street *et al.*[28] give the frequency response of such a system as

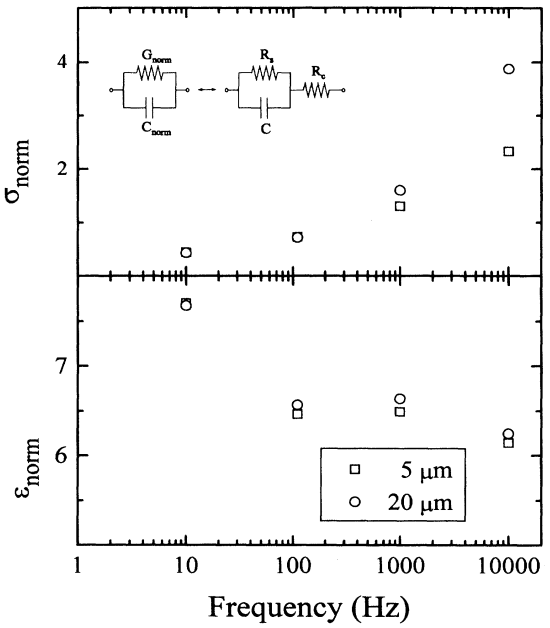

FIG. 1. Comparison of the normalized conductivities $\sigma_{\rm norm} = G_{\rm norm}d$ (where d is the thickness) and the normalized dielectric constants $\epsilon_{\rm norm} = C_{\rm norm}d$ as a function of frequency for two PS samples scaled for different thicknesses. The inset shows the equivalent circuits from which the parameter values can be extracted. See details in the text.

$$\frac{\left(1+\frac{R_c}{R_s}\right)\frac{1}{R_s}+R_c(\omega C)^2}{(1+\frac{R_c}{R_s})^2+(\omega R_c C)^2}+i\omega\frac{C}{(1+\frac{R_c}{R_s})^2+(\omega R_c C)^2}, \tag{5}$$

where R_s and R_c are the sample and contact resistances, respectively, and C the sample capacitance. Under the assumption that $R_s \gg R_c$, we get

$$G_{\rm norm} \approx \frac{1}{R_s},\ C_{\rm norm} \approx C \text{ when } \omega(R_cR_s)^{1/2}C < 1,$$
$$G_{\rm norm} \approx \omega^2 R_c C^2,\ C_{\rm norm} \approx C \text{ for } \omega R_c C < 1 < \omega(R_cR_s)^{1/2}C, \tag{6}$$

and

$$G_{\rm norm} \approx \frac{1}{R_c},\ C_{\rm norm} \approx \frac{C}{(\omega R_c C)^2} \text{ in the limit } 1 < \omega R_c C.$$

At low frequency, the measured conductance and capacitance reflect the sample conductivity and dielectric constant. However, at higher frequencies the measured conductance contains a term related to the contact resistance (6). This term causes the estimated conductivity of thin samples to be lower than its real value. The model predicts an ω^2 dependence of the ac conductivity in this frequency regime, a behavior that was observed in our samples.[29,30] In order to simplify the discussion, the data are corrected for the effect of the series resistance.

III. RESULTS

A. Conductivity

Figure 2 shows the frequency dependence of the real part of the conductivity at various temperatures. The solid line marks where the ac conductivities at different temperatures all merge. This line is a power law $\sigma'(\omega) \approx \omega^v$ with an exponent $v = 0.95 \pm 0.05$. Data below 200 K fall very close to it. As the temperature increases, a deviation from the line is observed. For each temperature, there is a temperature-dependent threshold frequency $\omega_c(T)$ (marked in the figure by arrows), which separates the high-frequency regime (the continuous line)

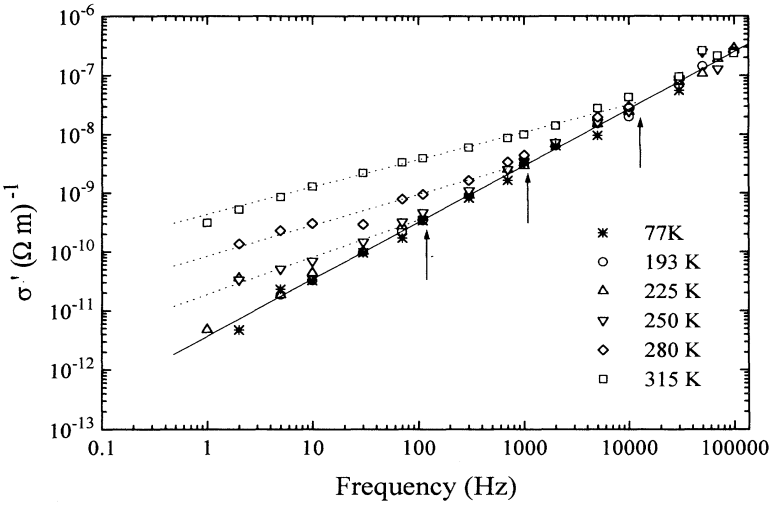

FIG. 2. Frequency dependence of the conductivity at different temperatures for a typical porous Si layer. The dashed and continuous lines in the figure have slopes of 1/2 and 0.95, respectively. The arrows mark the transition between the two frequency regimes.

and the low-frequency regime (the dashed lines). The threshold frequency is correlated with the dc conductivity at the same temperature $\sigma'(T)$, by $\omega_c(T) = A\sigma'(T)$, where A is a constant of the order of 100. The conductivity has different behavior in these two regions. At high frequency, it depends strongly on the frequency ($\sigma'(\omega) \approx \omega$) and is almost independent of the temperature. At low frequency $\sigma'(\omega) \approx \omega^{1/2}$, and a strong temperature dependence is observed. We note that a saturation of the conductivity to its dc value is not seen, even for frequencies well below the threshold. This indicates that in the measured frequency range we are still quite far from the dc limit.

The temperature dependence of the ac conductivity is compared with that of the dc conductivity in Fig. 3. The dc conductivity is activated above 200 K, with activation energy of 0.45 eV and a prefactor of $10^{-2}(\Omega\,\mathrm{m})^{-1}$. Below 200 K, it is almost temperature independent. The dependence of the ac conductivity on the temperature varies appreciably for different frequencies. Generally, at high temperatures the conductivity is activated while it saturates at low temperature. For sufficiently high frequencies no activation is observed, while in the same temperature range the dc conductivity changes exponentially. The temperature dependence in this saturation regime is shown in Fig. 4. The conductivity depends linearly on the temperature $\sigma'/\omega = T/T_0$, where T_0=4000 K.

Some preliminary conclusions can be drawn from these data. The dc conductivity might suggest that transport involves activation to a mobility edge. However, this is clearly not the case. An activated temperature dependence should then be observed for all frequencies.[13] The fact that at high enough frequencies the ac conductivity has only a weak temperature dependence implies that there is neither a gap in the density of states at the Fermi level, nor is activation to a mobility edge a relevant trans-

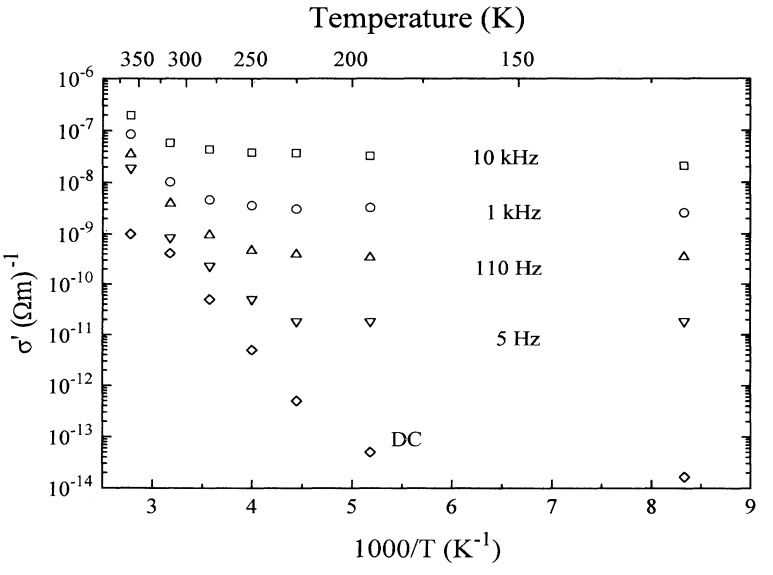

FIG. 3. The conductivity of a porous Si layer versus inverse temperature for different frequencies.

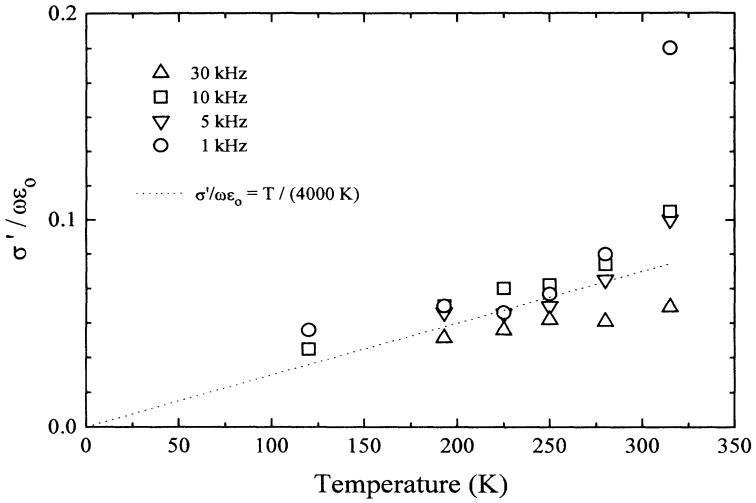

FIG. 4. The high-frequency ac conductivity of a PS sample at the saturation regime as a function of temperature. The conductivity is given in terms of an imaginary "dielectric constant" by dividing it by the measuring frequency and the vacuum permittivity. This is done in order to show data obtained at different frequencies on the same scale.

port mechanism. We are dealing with degenerate Fermi statistics and a finite density of states at the Fermi energy. The results in Figs. 2–4 are typical for hopping transport in the vicinity of the Fermi level.

B. Dielectric constant

The frequency dependence of the dielectric constant as derived from the capacitive component of the impedance, is shown in Fig. 5 for various temperatures. The most striking effect is the divergence of the dielectric "constant" at low frequencies, a feature that becomes more prominent as the temperature is increased. At high frequencies the dielectric constant saturates to a weakly temperature-dependent value $\epsilon(\infty, T)$. Figure 6 depicts this $\epsilon(\infty, T)$ for frequencies 1–30 kHz for which there exist reliable data after contact corrections. $\epsilon(\infty, T)$ is increasing linearly with temperature with a slope of (650 K)$^{-1}$. The extrapolated value of $\epsilon(\infty, T = 0)$ is 2.0±0.1.

The total dielectric response of our PS layers is described by

$$\epsilon = \epsilon_{el}(T) + \epsilon_l(T) + i\sigma''(\omega, T)/\omega. \quad (7)$$

Where $\epsilon_{el}(T)$ is the contribution due to polarization of inner electronic shells, $\epsilon_l(T)$ is the contribution from the lattice and the last term is due to mobile electrons. We assume that both electronic and lattice contributions are independent of frequency in our range of measurement. The temperature dependence observed in Fig. 6 arises mainly from the mobile electron term. The electronic and lattice contributions change only slightly with temperature, due to the thermal expansion of the lattice.

The limit $\epsilon(\infty, T = 0)$ gives the "lattice" and "atomic" contribution to the dielectric constant of PS. The value that we observe ($\epsilon \sim 2$) is in agreement with values of the refractive index obtained from ellipsometry measurements made at IR frequencies. At such high frequencies there is no contribution from the transport processes.

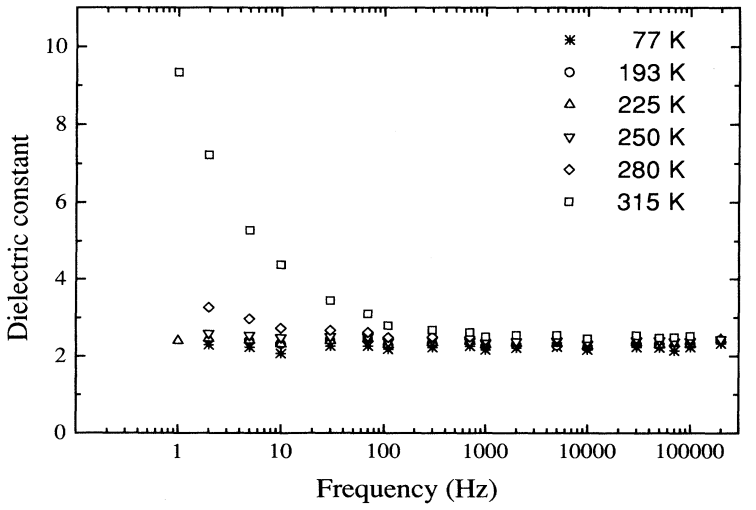

FIG. 5. The dielectric "constant" as a function of frequency at different temperatures.

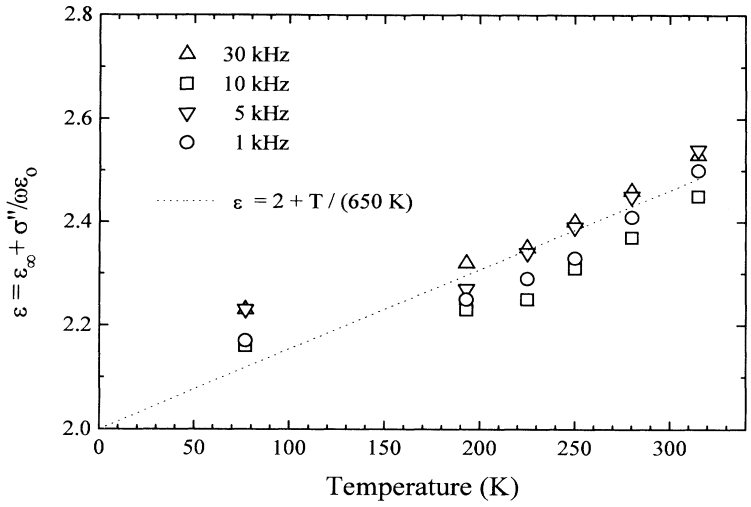

FIG. 6. The temperature dependence of the high-frequency dielectric constant.

The divergence of the dielectric constant at low frequencies in Fig. 5 deserves further clarification. Such dispersion is usually attributed to contact polarization (known as the Maxwell-Wagner phenomenon),[15,18] resulting from the parasitic capacitance of the contacts. We have neglected this capacitance in our interpretation of the data according to Fig. 1. Contact polarization effects, if present, lead to a thickness dependence of the effective dielectric constant.[31] This is not observed (see Fig. 1), and thus the divergence is not a contact effect.

We must look for another mechanism to explain the strong dispersion. As in the case of the ac conductivity, the frequency response of the dielectric constant can be divided to a regime of strong dispersion and the saturation regime. We note that there is a correlation between these two regimes of the dielectric constant and those observed in the ac conductivity measurements (Fig. 2). The same threshold frequency separates the low- and high-frequency regimes for the conductivity and the dielectric constant. The temperature dependence is also similar. At low frequencies both quantities depend strongly on temperature, while in the saturation regime a linear temperature dependence is observed. Figure 7 shows the frequency dependence of the real and imaginary parts of the dielectric constant. We have subtracted the high-frequency term from the real part in order to identify the electronic contribution. Both follow an approximate power law with the same power, as required by the Kramers-Kronig relations.[15] Again this observation suggests that parasitic impedances are not responsible for the divergence of the dielectric constant, but that this behavior is related to the same physical process which governs the anomalous diffusion observed in the low-frequency conductivity measurements.

C. Scaling properties

Figure 8 shows the normalized conductivity $\sigma'(\omega,T)/\sigma'(0,T)$ as a function of the normalized frequency

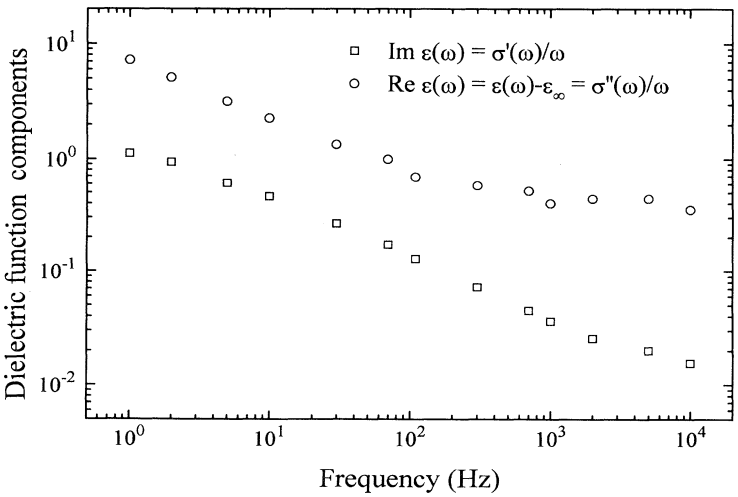

FIG. 7. The real and imaginary part of the dielectric susceptibility $\epsilon(\omega,T)-\epsilon(\infty,T)$, $\sigma'(\omega,T)/\omega$, for $T=315$ K with $\epsilon(\infty,T)=2.4$. Note that the real and imaginary part of the susceptibility are approximately parallel for a wide range of frequencies.

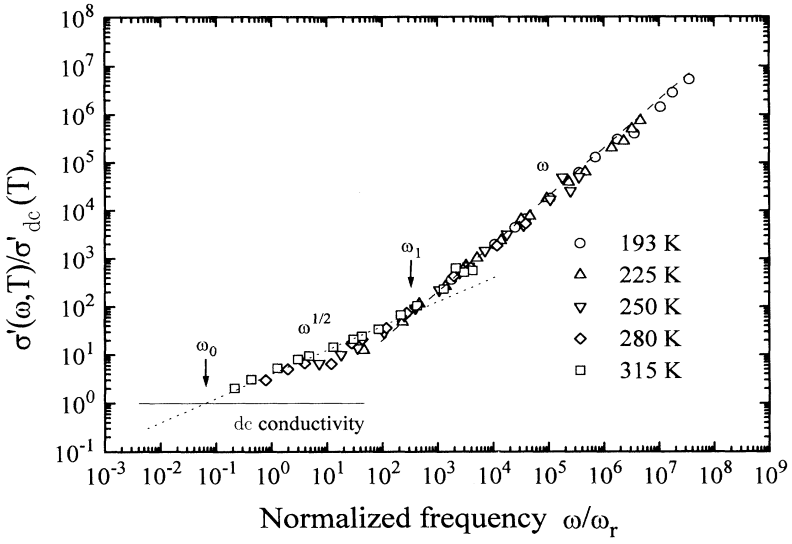

FIG. 8. Scaling picture for the real part of the ac conductivity, i.e., the scaled conductivity $\sigma'(\omega,T)/\sigma'_o(T)$ as a function of the normalized frequency $\omega/\omega_r(T)$. $\sigma'_o(T)$ and $\omega_r(T)$ are the dc conductivity and the dielectric relaxation time at the relevant temperature. The continuous line marks the dc conductivity. The short and long dashes note an $\omega^{1/2}$ and an ω^1 dependence, respectively. The arrows mark the two transitions.

$\omega/\omega_r(T)$, where $\omega_r(T)$ is the dielectric relaxation frequency $\sigma'(0,T)/\epsilon$. All temperature data fall on the same curve, suggesting a simple scaling law for the ac conductivity. Similar scaling can also be found for the dielectric constant (see Fig. 9).

The scaling shows that there is a relation between the dc and high-frequency conductivities, even though they have completely different behavior as a function of temperature and frequency. It suggests that the same transport mechanism is responsible for the conductivity in these two regimes. Moreover, since the dielectric constant can also be scaled with respect to the dc conductivity, we have additional evidence that the strong dispersion is related to the low-frequency transport properties.

Scaling relations are predicted by most of the hopping theories.[14,23,24,32–34] The mere existence of the scaling does not identify the physical mechanism of the transport. However, our experimental scaling function is different from what is usually observed in hopping systems. It is seen that we have, in addition to the usual crossover from frequency-independent to frequency-dependent behavior, a crossover from a ω^u to a ω^v law with $u \approx 0.5$ and $v \approx 1$. We see in this evidence that there is a crossover from a frequency dependence due to the fractal character of the porous material to a "conventional" ω^v law due to a large distribution of activation energies. We shall explore this idea in detail in the sections below.

IV. THEORETICAL DESCRIPTION

The transport mechanism that is suggested from the experimental observations is activated hopping on a fractal with fluctuating activation energies. In our theoretical description, we start with a summary on what is known about random walk on fractals and its consequences for the ac conductivity. We derive a scaling law describing the dc-ac crossover in a fractal with finite correlation

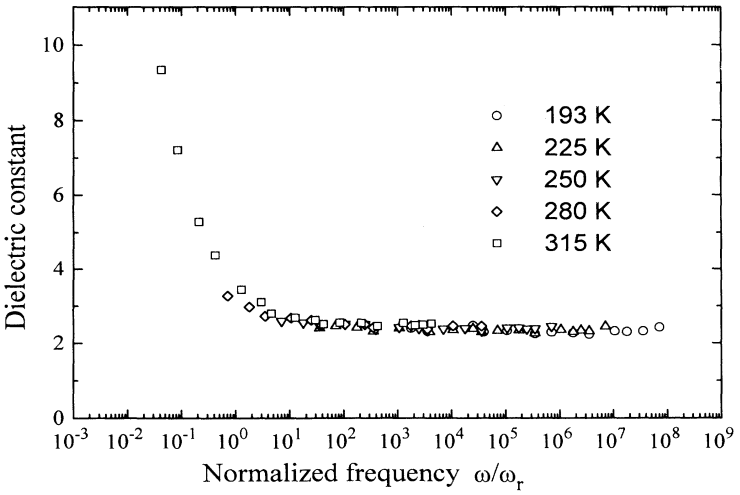

FIG. 9. Scaling picture for the ac "dielectric constant," i.e., the dielectric constant as a function of normalized frequency.

length. Turning to the fluctuating activation energy aspect, we consider the pair approximation. This is the simplest scheme describing the ac conductivity in such a situation. By combining the two aspects, we obtain a simple phenomenological scaling formula which describes the crossover from the fractal to the disorder-dominated frequency region. Next, we substantiate these findings by means of the effective-medium approximation (EMA) applied to an activated hopping model on a percolating lattice.

A. Random walk of carriers and ac conductivity in fractals

The quantity of interest is the complex dynamic conductivity $\sigma(\omega)$, the real part of which is the ac conductivity. If the ac response is due to the diffusive motion of carriers with charge e, the generalized Einstein relation[14] applies in the form

$$\sigma(\omega) = e^2 \frac{\partial n}{\partial \mu} D(\omega). \tag{8}$$

Here $D(\omega)$ is the generalized frequency-dependent diffusivity, n the number of carriers, and μ the chemical potential.[35] In systems with a finite diffusion coefficient D, we have $\lim_{\omega \to 0} D(\omega) = D$.

For noninteracting carriers the diffusive motion of the carriers is described by a single-particle random walk. In this case, $D(\omega)$ is the Laplace transform $D(p = i\omega + 0)$ of the velocity autocorrelation function, which, in turn, is related to the Laplace transform of the mean square distance $\langle r^2(t) \rangle$ walked by the particle by[36]

$$\langle r^2(p) \rangle = 6D(p)/p^2. \tag{9}$$

Normal diffusion is the case if $\langle r^2(t) \rangle$ increases *linearly* with time, i.e.,

$$\langle r^2(t) \rangle = 6Dt, \tag{10}$$

where D is the diffusion coefficient. By (9) this implies a frequency independent $D(\omega)$. *Anomalous diffusion*[23,24,37,38] is present if $\langle r^2(t) \rangle$ increases *sublinearly* with t, for example, according to

$$\langle r^2(t) \rangle \propto t^{2/d_W}, \tag{11}$$

where $d_W > 2$ is the "random walk dimension" or "diffusion exponent." By (8) and (9) this implies an anomalous frequency-dependent conductivity of the form $\sigma(\omega) \propto (i\omega)^u$ with

$$u = 1 - 2/d_W. \tag{12}$$

A crossover according to (2) with scaling function (3) is equivalent to a transition from anomalous diffusion for times $t < t_0$ to normal diffusion for $t > t_0$ with $t_0^{-1} \propto x_0$.

A *fractal*[39] is a self similar geometrical object in which the mass M of a region of diameter L scales as $M(L) \propto L^{\bar{d}}$, $\bar{d} < d$, where d is the dimension of the embedding space and $\bar{d}$ is the *Haussdorff* or *fractal* dimension. The x-ray (or neutron) scattering intensity of materials with fractal properties varies with wave number q as $i(q) \propto q^{-\bar{d}}$. In fact, such anomalous small-angle scattering has been observed in the type of PS material discussed in this paper[10–12] (see below).

It has been shown by Alexander and Orbach[37] that a random walk on a fractal implies a sublinear time dependence of $\langle r^2(t) \rangle$ according to (11) with

$$d_W = 2\bar{d}/\tilde{d}, \tag{13}$$

where $\tilde{d}$ is the *spectral* or *fracton* dimension, and we have $\tilde{d} < \bar{d}$. The fracton dimension is determined by the vibrational density of states $N(\omega)$ of the fractal which is proportional to $\omega^{\tilde{d}-1}$. Accordingly the temperature dependence of the specific heat is given by $C(T) \propto T^{\tilde{d}}$.

An example of a fractal which has been studied extensively by numerical and analytical theoretical work is a *percolating lattice.*[38,40] In the bond percolation problem, bonds with concentration x are distributed randomly on a d-dimensional lattice. In the site percolation problem, impurities are distributed at random with concentration x and are treated as connected if they occupy nearest-neighbor sites. In both cases, below a critical concentration x_c, only connected clusters with finite size exist. At a critical concentration x_c an infinite cluster appears which is called the percolation cluster. For $d = 3$ it has a fractal dimension $\bar{d} \approx 2.5$ and a spectral dimension $\tilde{d} \approx 1.33$. This gives the random walk dimension as $d_W \approx 3.77$ and correspondingly $u \approx 0.47$. d_W has also been determined independently by numerical simulation (see Ref. 38) to be in the range $3.45 \leq d_W \leq 4.0$. These numbers apply both for site and for bond percolation.

In percolating systems, the presence of finite clusters even for $x > x_c$ leads to a slightly larger value u as compared to relation (12).[41] Since we are not dealing with a percolating system, but with a porous material, which is more similar to the "backbone" of the infinite percolation cluster and does not contain isolated clusters of material, we disregard this effect.[42]

For $x > x_c$, one can define a correlation length ξ. On length scales smaller than ξ the structure of the percolating network looks like the critical cluster, on a scale larger than ξ it looks homogeneous. ξ obeys the scaling relation

$$\xi/a \approx |(x - x_c)/x_c|^{-\nu}, \tag{14}$$

where a is the microscopic length scale (average hopping distance). In $d = 3$, we have $\nu = 0.9$. If $\sqrt{\langle r^2(t) \rangle}$ becomes larger than ξ, one has a crossover from anomalous diffusion with $d_W \approx 4$ to normal diffusion at a characteristic time $t_0 = \xi^2/D$. The diffusion constant D vanishes according to $D \propto (x - x_c)^{\tilde{\mu}}$ with $\tilde{\mu} \approx 1.5$ in $d = 3$.[43]

The concept of a correlation length can be generalized. Let us consider a system which on length scales smaller than ξ has fractal properties and on length scales larger than ξ is homogeneous. The mean square distance in such a system behaves as

$$\frac{1}{6}\langle r^2(t) \rangle = \begin{cases} Dt_0 \, (t/t_0)^{2/d_W}, & t \ll t_0 \\ Dt, & t \gg t_0, \end{cases} \tag{15}$$

where, again,

$$t_0 = \frac{1}{\omega_0} = \xi^2/D. \tag{16}$$

Using (9), we obtain for the dynamic diffusion coefficient

$$D(\omega) = \begin{cases} D, & \omega \ll \omega_0 \\ D\,(i\omega/\omega_0)^u, & \omega \gg \omega_0, \end{cases} \tag{17}$$

with $u = 1 - 2/d_W$. Porous Si is such a system, because on a macroscopic length scale it is homogeneous.

B. Fluctuating activation energies and Pair approximation

In what follows, we consider activated hopping between sites i and j separated by an activation barrier E_{ij} and a spatial distance r_{ij}. The hopping probability per unit time is assumed to be of the form

$$W_{ij} = W(E_{ij}) = \nu_0 \exp\{-E_{ij}/k_BT\}. \tag{18}$$

ν_0 is the attempt frequency. For classical barrier hopping, ν_0 should be of the order of a phonon frequency $\nu_p \approx 10^{12}$ Hz. For phonon-assisted tunneling between localized states, there is an additional tunneling factor $\nu_0 = \nu_p \exp\{-2r_{ij}/\tilde{\xi}\}$, where $\tilde{\xi}$ is the localization length.[44]

The simplest model for the ac conductivity due to such a process is the pair approximation[13,25] in which carriers are assumed to hop between isolated pairs of sites. The frequency-dependent diffusivity is given by

$$D(\omega) \approx \left\langle r_{ij}^2 \left[\frac{1}{W_{ij}} + \frac{1}{i\omega}\right]^{-1} \right\rangle, \tag{19}$$

where $\langle\,\rangle$ means an average over a large number of pair configurations. In the case of a uniform barrier distribution $P(E_{ij})$ =const= $1/E_0$, we have[13]

$$D(\omega) = a^2 i\omega \frac{k_BT}{E_0} \ln\left[1 + \frac{\nu_0}{i\omega}\right], \tag{20}$$

where a is the mean pair site separation.

Identifying E_0 with the inverse energy level density,[13]

$$E_0 \approx \frac{1}{N(E_F)a^3}, \tag{21}$$

we have for the ac conductivity in the frequency regime $\omega \ll \nu_0$ (Ref. 13)

$$\sigma'(\omega) = e^2 a^5 N(E_F)^2 k_BT \omega \frac{\pi}{2}. \tag{22}$$

C. Combined phenomenological scaling law

We assert that below a crossover frequency ω_1, the ac conductivity is determined by the fractal properties of the system, i.e., $D(\omega)$ is given by expression (17), and above ω_1, it is governed by the fluctuating activation energies.

The value of ω_1 can be estimated by requiring that $\sqrt{\langle r^2(t_1)\rangle}$ (with $t_1 = \omega_1^{-1}$) is of the order of the microscopic length scale a of the system. Setting $a^2 = \frac{1}{6}\langle r^2(t_1)\rangle$ in equation (15) with $t_1 < t_0$, and using (16), we obtain

$$t_1^{-1} = \omega_1 \approx \omega_0\,(\xi/a)^{d_W}\,. \tag{23}$$

By this relation we are able to estimate the ratio ξ/a, which is an important structural parameter.

If we assume that at high frequencies the ac conductivity is given by expression (22) with $\omega \ll \nu_0$, we can write down the scaling law

$$\sigma'(\omega) = \sigma'(0) f\left(\frac{\omega}{\omega_r'}\right). \tag{24}$$

The reference frequency

$$\omega_r' = D/a^2 = \sigma'(0)/a^2e^2N(E_F), \tag{25}$$

can be identified with a dielectric relaxation frequency. The universal function is given by

$$f(x) \approx \begin{cases} 1, & x \ll x_0 \\ (x/x_0)^u, & x_0 \ll x \ll x_1 \\ x/\beta E_0, & x \gg x_1, \end{cases} \tag{26}$$

with $\beta = [k_B\langle T\rangle]^{-1}$, where $\langle T\rangle$ is a mean value of the experimentally relevant temperature. $x_0 \approx \omega_0/\omega_r'$ is the lower and $x_1 \approx x_0(\xi/a)^{d_W}(\beta E_0)^{d_W/2}$ is the higher crossover point. The latter relation for ω_1 has a different prefactor than relation (23). However, in determining the ratio ξ/a this amounts to a factor $(\beta E_0)^{1/2}$, which is typically of order unity.

D. Effective-medium approximation

Although we are able to explain the salient features of the data qualitatively by such semiphenomenological considerations, we would like to have a model to calculate explicitly the dynamic conductivity across the whole frequency range, from dc through the fractal $\sigma' \propto \omega^{1/2}$ frequency dispersion to the regime of validity of the pair approximation. Such a model is provided by a percolating lattice on which carriers perform activated hopping with a broad distribution of activation energies. This model can be solved in the effective-medium approximation.

The effective medium[19,45,14] or coherent potential[46] approximation is a mean field theory for the dynamics of excitations in disordered systems. The idea is to replace the fluctuating hopping rates W_{ij} by a uniform, but frequency-dependent $W_M(\omega)$ (effective medium). Then one picks a particular pair ij, replaces again $W_M(\omega)$ by W_{ij} and requires that this operation should have—on the average—no effect on the effective medium. The "amorphous" version of the EMA (Refs. 47–52) is reviewed in Refs. 24 and 53. In the present study we utilize the lattice version of the EMA,[54–56] in which the effective medium

is taken to be a simple cubic lattice.

The self consistent EMA equation derived in Refs. 54–56 has the form

$$\left\langle \frac{W_M(\omega) - W_{ij}}{1 - \frac{2}{ZW_M(\omega)} Q_M(\omega)\,[W_M(\omega) - W_{ij}]} \right\rangle = 0. \quad (27)$$

Here, $\langle\,\rangle$ is a configuration average, Z (= 6 for the simple cubic lattice) is the coordination number, $Q_M(\omega) = 1 - i\omega G_M(\omega)$, and $G_M(\omega)$ is the diagonal lattice Green's function[57] of the medium. Equation (27) can be rewritten as

$$W_M = \left\langle \frac{W_{ij}}{1 - \frac{2}{ZW_M(\omega)} Q_M(\omega)\,[W_M(\omega) - W_{ij}]} \right\rangle . \quad (28)$$

The frequency-dependent diffusivity is given by

$$D(\omega) = a^2\, W_M(\omega), \quad (29)$$

where a is now identified with the lattice constant of the effective medium.

In the dc limit $\omega \to 0$ the EMA equation (28) takes the form

$$1 = \left\langle \frac{W_{ij}}{W_M(0)[1 - \frac{2}{Z}] + \frac{2}{Z} W_{ij}} \right\rangle . \quad (30)$$

Here, $W_M(0) = W_M(\omega = 0)$.

Let us now study the EMA expression in the limit, $\omega \gg W_M(\omega)$. In this limit, the Green's function of the medium $G_M(\omega)$ can be expanded as

$$i\omega G_M(\omega) = 1 - \frac{ZW_M(\omega)}{i\omega} + \cdots . \quad (31)$$

Inserting the leading terms into (28) gives

$$W_M(\omega) = i\omega \left\langle \frac{W_{ij}}{2W_{ij} + i\omega[1 - \frac{2W_M(\omega)}{i\omega}]} \right\rangle \approx \langle W_{ij} \rangle \quad \text{for } \omega \to \infty. \quad (32)$$

Replacing the interior of the square bracket in the denominator of Eq. (32) by unity, we obtain essentially Eq. (19), namely, the pair approximation. Therefore, the EMA can be considered as a generalized pair approximation[51] which interpolates between the Bruggeman EMA (Ref. 19) value of the dc conductivity and (19). The "amorphous" version of the EMA,[47–52] which has been checked by us to give almost the same results as the lattice version used presently, compares well with numerical simulations of disordered hopping systems.[14,49] In disordered systems, it predicts a strong frequency dispersion for the case that the dc value of W_M is lower by orders of magnitudes than the $\omega \to \infty$ value[58] given by Eq. (32). In the case of a constant distribution of activation energies one obtains approximately a behavior according to (1), where the exponent v lies between 0.8 and 1.

It is worthwhile to note that in the region of the strong frequency dependence the EMA predicts a weaker variation of σ' with ω than the pair approximation. The two approaches give exactly the same results only in the vicinity of the saturation. We shall see in our numerical calculations (Fig. 10) that the discrepancy between EMA and the pair approximation is accompanied by a slightly nonuniversal behavior in the sense of (24) and (26).

1. *Percolating lattice without fluctuating hopping rates*

Before we consider our model with fluctuating activation energies, we remind the reader of the EMA description of a percolating lattice *without* fluctuating W_{ij}.[54–56] Consider a bond percolation problem in which for connected sites i,j we have $W_{ij} = W$, and for disconnected sites $W_{ij} = 0$. From (30), we obtain for the dc conductivity

$$W_M(0) = \frac{x - x_M}{1 - x_M} W, \quad (33)$$

where $x_M = 2/Z$ is the EMA percolation threshold. We

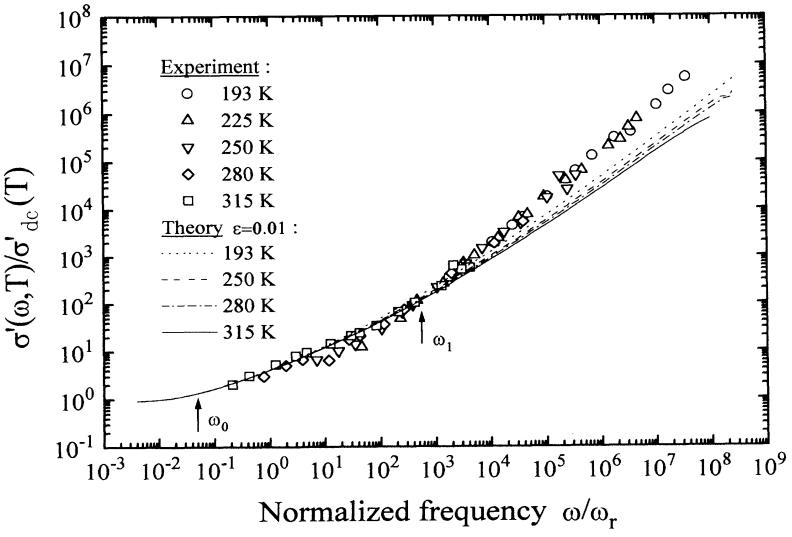

FIG. 10. Comparison between the experimental (symbols) and theoretical (lines) scaling curves. The theory curves correspond to activated hopping on a percolating lattice near its percolation threshold treated in the effective-medium approximation (EMA, see text).

see that in EMA, $\tilde{\mu} = 1$.

The full EMA equation for this model reads

$$W_M(\omega) = x \frac{W}{1 - \frac{x_M}{W_M(\omega)} Q_M(\omega) [W_M(\omega) - W]}. \quad (34)$$

In the literature[55,56] it has been shown that the EMA predicts critical behavior in the vicinity of the EMA threshold with $u = 1/2$ and, correspondingly, $d_W = 4$. The correlation length exponent is $\nu = 1/2$.

In contrast to $\tilde{\mu}$ and ν, the exponent u is almost the same as the exact value obtained from simulations. On the other hand, it agrees nicely with the frequency exponent that we observe in the fractal frequency domain of the ac conductivity of PS.

2. *Percolating lattice with fluctuating hopping rates*

The EMA equation for fluctuating W_{ij}, according to (18) and with barrier distribution $P(E)$ on a percolating lattice, which is characterized by the bond concentration $x \equiv x_M(1+\epsilon)$, takes the form

$$W_M(\omega) = x \int_0^\infty dE P(E) \times \frac{W(E)}{1 - \frac{x_M}{W_M(\omega)} Q_M(\omega) [W_M(\omega) - W(E)]}. \quad (35)$$

a. dc conductivity. The dc limit of (35) takes the form

$$1 = x \int_0^\infty dE P(E) \frac{W(E)}{(1 - x_M) W_M(0) + W(E)}. \quad (36)$$

Since we expect $W_M(0) \to 0$, for $\epsilon \to 0$, we put

$$W_M(0) = W_0 \epsilon^{\tilde{\mu}} \quad (37)$$

and expand the right-hand side of (36) in powers of ϵ. We obtain a nontrivial solution for $\tilde{\mu} = 1$ with

$$W_0 = p_M \left\langle \frac{1}{(W(E)} \right\rangle^{-1}, \quad (38)$$

where $p_M = x_M/(1 - x_M) = 1/2$ for $Z = 6$. The angular brackets $\langle\rangle$ now and in the following mean an average over the distribution $P(E)$ only. The physical meaning of this result is that hopping along the backbone of the percolation cluster samples all "conductances" W_{ij} in series.

Inserting the (normalized) uniform distribution function

$$P(E) = \begin{cases} 1/E_0, & E \le E_0 \\ 0, & E > E_0, \end{cases} \quad (39)$$

we obtain for W_0 [and hence for $W_M(0)$]:

$$W_M(0) = \epsilon W_0 = \epsilon p_M \frac{\nu_0 E_0}{k_B T} [\exp\{E_0/k_B T\} - 1]^{-1} \approx \epsilon \frac{\nu_0 E_0}{k_B T} \exp\{-E_0/k_B T\}. \quad (40)$$

Thus we identify E_0 as the apparent activation energy of the measured dc conductivity.

The correlation length exponent is $\nu = 1/2$ (see Appendix).

b. Low-frequency ac conductivity. It is shown in the Appendix that in the limit $\epsilon = 0$, we obtain for $\omega \to 0$,

$$W_M(\omega) = W_1 (i\omega)^u, \quad (41)$$

with $u = 1/2$ and $W_1 \approx W_0^{1/2}$.

c. Crossover frequencies. For the dc-ac crossover frequency ω_0, we have explicitly (see appendix):

$$\omega_0 = \epsilon^2 W_0. \quad (42)$$

The crossover frequency ω_1 into the high-frequency regime is obtained as

$$\omega_1 \approx W_0/(\beta E_0)^2 = (\xi/a)^4 \omega_0/(\beta E_0)^2. \quad (43)$$

The scaling behavior of this expression agrees with our general scaling relation (23) to within a prefactor. The latter is different from that obtained from the phenomenological relation (26), but, again, for determining ξ/a only a factor of order unity is involved.

V. COMPARISON OF THEORY WITH EXPERIMENT

In the following, we try to extract physically relevant parameters from a comparison of our experimental data with the theoretical considerations. To facilitate this, let us collect the formulas for the dc and high-frequency conductivity. As stated above, we may identify the density-of-states parameter E_0 with the activation energy of the measured dc conductivity, which is $E_0 = 0.45 \pm 0.05$ eV. Combining (29) with (41) and using the Einstein relation (8) with $\partial n/\partial \mu = N(E_F)$, we find for the dc conductivity

$$\sigma(0) = \sigma_0 \exp\{-E_0/k_B T\}, \quad (44)$$

with $(\beta = 1/k_B T)$

$$\sigma_0 = N(E_F) e^2 a^2 \frac{1}{2} \epsilon \beta E_0 \nu_0. \quad (45)$$

For high frequencies, we obtain from the pair approximation (32) in the regime $w \ll \nu_0$ the real and imaginary parts of $\sigma(\omega)$ as

$$\sigma'(\omega) = N(E_F) e^2 a^2 \omega \frac{\pi}{2\beta E_0}, \quad (46)$$

$$\sigma''(\omega) = N(E_F) e^2 a^2 \omega \frac{1}{\beta E_0} \ln(\nu_0/\omega). \quad (47)$$

Both real and imaginary parts of the conductivity depend linearly on the temperature and frequency as observed in the experiments. Moreover, from the ratio between the real and imaginary part of $d\sigma/dT$, we obtain an attempt frequency of $\nu_0 \approx 10^{10}$ s^{-1}. This is a very reasonable value, because it should be the product of a typical phonon frequency and a tunneling factor.

In order to evaluate the density of states at the Fermi level, we use the temperature dependence of the ac conductivity and combine formulas (21) and (46) to obtain $N(E_F) \approx 10^{19}$ eV^{-1} cm^{-3} and $a \approx 50$ Å. The value of a is of the order of the typical crystallite size, confirming that the hopping occurs from one crystallite to the other. $N(E_F)$ appears to be rather large for a Fermi level in the forbidden gap of all the crystallites. However, the large internal surface area of the PS (≈ 500 m^2/cm^3) may cause a high density of surface states. Taking reasonable numbers for the surface states density ($\approx 10^{12}$ cm^{-2}eV^{-1}), we just arrive at our measured value for $N(E_F)$. Moreover, the energy spectra of the different quantum wells are shifted with respect to one another due to partial charging effects either by doping or by different chemical bonding on the surface. Thus, the effective density of states near the Fermi level involves the local state densities near the conduction or valence bands of particular crystallites.

We now discuss the fractal properties of PS. The fractal dimension $\bar{d}$ has been determined directly by small-angle x-ray[10,11] and neutron[12] scattering as a function of porosity. In a limited range of wave numbers the scattering intensity varies according to $i(q) \propto q^{-\bar{d}}$ as expected. The parameter $\bar{d}$ has been shown[11] to take values from $\bar{d} \approx 3$ at 55% porosity, decreasing to $\bar{d} \approx 2$ at 68% and $\bar{d} \approx 1$ at 85 % porosity. Since our samples have a porosity of about 60–70 %, we assert that $\bar{d} \approx 2$. From the experimental value of $u \approx 0.5$ in the low-frequency scaling regime, we conclude from relations (12) and (13) that the spectral dimension of our material is $\tilde{d} \approx 1$. This value seems to be rather small, because in other fractal materials $\tilde{d}$ takes values lying in the range 1.2 to 1.5.[59,60] However, we think this is still compatible with the estimates performed above, because the fractal dimension is very sensitive to the porosity and the error in the latter quantity is rather large.

We next estimate the degree of fractality measured by the parameter ξ/a, the ratio of the correlation length to the mean hopping distance. By the scaling relation (23) this can be obtained from the ratio of the two crossover frequencies. Since in our data $\omega_1/\omega_0 \approx 10^4$, we obtain with $d_W = 4$ the parameter $\xi/a \approx 10$. A similar result is obtained in EMA for which $\xi/a = \epsilon^{-1/2}$ applies. Together with our value of a, we arrive at $\xi \approx 500$ Å. From the small-angle x-ray data[11] one deduces a value of ξ which lies roughly between 100 and 1000 Å.

We now compare the predictions of the EMA with our data in more detail. In Fig. 10, we show the scaling function of Fig. 8 together with the scaling function obtained from the EMA using $\epsilon = 0.01$ and $E_0 = 0.42$ eV. In the low-frequency regime, the data are described very well by the theory. In the high-frequency regime $\omega > \omega_1$ the calculated curves deviate from the measured ones: The frequency dependence predicted by the EMA is weaker than $\sigma' \propto \omega$, the calculated crossover is more smeared out than the measured one, and the calculations show a nonuniversal temperature dependence not observed in the experimental data. This behavior is due to the fact that in the frequency regime $\omega_1 < \omega < \langle W_{ij} \rangle$ the EMA does not describe pair hopping but hopping within clusters of more than two sites. The number of these sites is the larger the lower the frequency is and becomes infinity in the dc limit. Only at very high frequencies $\omega \approx \langle W_{ij} \rangle$, where both approaches predict a saturation of $\sigma'(\omega)$, the EMA is equivalent to the pair approximation.

We conclude from the linear frequency dependence of the experimental data that in PS hopping among clusters which contain more than two sites (i.e., Si crystallites) is suppressed in the high-frequency regime.

VI. DISCUSSION

In the Introduction, we pointed out the high resistivity of PS and discussed some possible reasons for that. We would now like to draw some conclusions about this question in light of the results presented above. As we have already stated, the temperature dependence of the conductivity (especially at high frequencies) implies that the transport mechanism is hopping in the vicinity of the Fermi level. The ≈ 0.5 eV activation energy of the dc conductivity has nothing to do with thermal generation of carriers accoss an energy gap. Quite contrary, we find a high density of states at the fermi level $N(E_F) \approx 10^{19}$ eV^{-1}cm^{-3}. One could argue that the dc current might be carried in a small portion of the sample, composed of intrinsic c-Si "needles" (with no quantum confinement), while the ac conductivity arises from polarization currents in disconnected particles. However, the scaling proves that the same transport mechanism is responsible for both the high frequency and the dc conductivity. Thus, such explanations based on the inhomogeneous structure of the sample can be ruled out.

There is one important difference between our data and the behavior usually observed in amorphous materials. This is the intermediate region, in which the conductivity follows an $\omega^{1/2}$ law. In homogeneous disordered systems there is only one crossover from a frequency-independent conductivity (the dc limit) to a ω^v regime (with $v \approx 0.8 - 0.9$). In our system, two crossovers are observed: dc to $\omega^{1/2}$ and $\omega^{1/2}$ to ω^1. This is related to the fact we emphasized above, that the ac conductivity is caused by hopping of charged carriers and not by polarization of atoms or metallic particles. The electrons perform a random walk in the disordered fractal system in the presence of the electric field. They will pass a certain distance before the field changes its polarity. For higher frequencies the distance walked will be shorter. In a homogoneous systems only one typical distance scale exist, namely, the average hopping length. In PS samples, two typical length scales can be found: The hopping length, which is comparable to the typical crystallite size, and the correlation length, which is the typical scale of the inhomogeneity. This is the reason for the two transitions

observed in our experiments. These two length scales are also observed in small-angle x-ray scattering. In these experiments, a fractal structure is observed for length scales between a few hundreds of Å and up to $\approx$ 1000 Å (the upper limit is given the experimental limitations). At shorter length scales, the typical Si particles sizes can be deduced to be in the range of a few tens of Å. Both these values are quite compatible with our estimates of the hopping distance ($\approx$ 50 Å) and the correlation length of the percolating system ($\approx$ 500 Å).

One of the most interesting aspects of the present study is that we can determine directly the random walk dimension d_W from the frequency dependence of the ac conductivity. Our value of $d_W = 4$ implies a relation $\tilde{d} = \bar{d}/2$ between the spectral and the fractal dimension. As stated above, $\tilde{d}$ in other fractal materials is always $\geq$1.2. It should be interesting to directly determine $\tilde{d}$ by inelastic neutron scattering,[60] in order to investigate, whether this applies also to PS. If so, the fractal dimension should be $\geq$ 2.4. The measurements of small-angle x-ray scattering of Vezin *et al.*[11] give a smaller value. A possible reason for this could be that the fractal seen by the x rays might have a slightly different topology than the conducting network.

Our use of a percolating network to model the PS structure is due to its simplicity. We do not believe that the real strucutre of the Si skeleton is similar to this artificial model. The scaling relation (24), (26) proposed by us applies to any fractal with finite correlation length. Nevertheless, in terms of diffusion and conductivity, it seems that the properties of the real system are reproduced by this simple model.

In the above discussion, we ignored the possible influence of Coulomb interactions on the ac conductivity. It is known that these effects are important in the dc transport.[8] The field dependence of the dc conductivity has been interpreted in terms of hopping in the vicinity of charged centers. It was further argued, that these centers are the crystallites themselves and that the transfer from one crystallite to another involves a Coulomb-Blockade type energy. Such effects will also influence the ac conductivity. However, a detailed analysis of them is very difficult. The role of Coulomb interactions in the ac conductivity of disordered systems has been examined only for the case of the Coulomb gap[61] using the pair approximation. For states within the gap, it was found that the conductivity follows an ω^s law where s is a bit larger than in the noninteracting case. Furthermore, the temperature dependence in the high-frequency regime is weaker than linear. However, the analysis performed for the Coulomb-gap cannot be applied directy to our case. We believe, that our main conclusions about hopping in the vicinity of the Fermi level and the role of the fractal structure in the low-frequency transport are still valid in a mean-field sense.

To summarize, we have shown that the transport mechanism in microporous Si is governed by hopping at the Fermi level. The density of states at the Fermi level is very high, almost comparable to what is found in unhydrogenated a-Si. The geometrical constraints imposed by the fractal structure of the Si skeleton alter the transport properties by reducing further the dc conductivity, and giving rise to additional dispersion at low frequencies. Thus, a relation between the electrical and the structural properties is obtained.

APPENDIX

In this appendix, we show how to obtain the low-frequency exponent u in EMA for the combined fractal and disordered model.

For reaching this goal, we have to include the Green's function,

$$G_M(\omega) = \sum_{\mathbf{k}} \frac{1}{i\omega + W_M(\omega)[Z - 2\cos(k_x a) - 2\cos(k_y a) - 2\cos(k_z a)]}, \tag{A1}$$

explicitly into our consideration. The summation goes over the first Brillouin zone. For $\epsilon = 0$, we make the ansatz

$$W_M(\omega) = W_1(i\omega)^u, \tag{A2}$$

with $u < 1$. From this, it follows in the $\omega \to 0$ limit,

$$G_M(\omega) = \frac{g_0}{W_M(\omega)} = \frac{g_0}{W_1}(i\omega)^{-u}, \tag{A3}$$

with

$$g_0 = \sum_{\mathbf{k}} \frac{1}{Z - 2\cos(k_x a) - 2\cos(k_y a) - 2\cos(k_z a)} . \tag{A4}$$

For $Z = 6$, we have $g_0 = 0.26$.[57] Setting $x = x_M$ and defining $q_M = (1 - x_M Q_M)/x_M$, we rewrite the EMA self consistency equation (35) in the form

$$\left\langle \frac{i\omega G_M(\omega) - q_M W_M(\omega)/W(E)}{1 - i\omega G_M(\omega) + q_M W_M(\omega)/W(E)} \right\rangle = 0. \tag{A5}$$

Since in the low-frequency limit the denominator is finite and tends towards unity, we have

$$\langle i\omega G_M(\omega) - q_M W_M(\omega)/W(E) \rangle = 0, \tag{A6}$$

from which we obtain $u = 1/2$ and

$$W_1^2 = W_0 g_0. \tag{A7}$$

The crossover frequency (at finite ϵ) from dc to ac behavior can be estimated by putting $|W_M(\omega_0, \epsilon = 0)| = W_M(\omega = 0, \epsilon)$ with the result

$$\omega_0 = \epsilon^2 W_0/g_0 \approx \epsilon^2 W_0 = \epsilon D/(a^2). \tag{A8}$$

Comparing with (16), we find

$$\xi/a = \epsilon^{-1/2}, \tag{A9}$$

i.e., we have for the correlation length exponent in EMA $\nu = 1/2$. This result can be obtained directly from the EMA equation (35) for $\epsilon < 0$ by identifying ξ^2 with $D(\omega)/i\omega$.

An estimate for the crossover frequency ω_1 from the fractal frequency regime to that determined by the fluctuating activation energies can be obtained from the regime of validity of relation (A6). The crossover starts at frequencies above which $i\omega G_M(\omega) - q_M W_M(\omega)/W(E)$ is no more a small number (i.e., $\ll 1$). This expression obtains values of the order of one if $W_M(\omega) = W_1(i\omega)^{1/2}$ becomes comparable with the smallest transition rate, which is $W(E) = \nu_0 \exp\{-E_0\}$. From this we obtain

$$\omega_1 \approx W_0/(\beta E_0)^2 = (\xi/a)^4 \omega_0/(\beta E_0)^2. \tag{A10}$$

At the end let us remark that for our numerical calculations, we replaced the lattice Green's function (A1) by the approximate expression (Hubbard approximation[57]),

$$G_0(p) = \frac{2}{i\omega + ZW_M + \sqrt{(i\omega + ZW_M)^2 - Z^2 W_M^2}}. \tag{A11}$$

In this approximation the relations derived above hold with $g_0 = 2/Z$, which is equal to $1/3$ for $Z = 6$.

[1] L. T. Canham, Appl. Phys. Lett. **57**, 1046 (1990).
[2] C. Pickering, M. I. J. Beale, D. J. Robbins, P. J. Pearson, and R. Greef, J. Phys. C **17**, 6535 (1984).
[3] A. G. Cullis and L. T. Canham, Nature **353**, 335 (1991).
[4] V. Lehman and U. Gösele, Appl. Phys. Lett. **58**, 856 (1991).
[5] M. I. J. Beale, J. D. Benjamin, M. J. Uren, N. G. Chew, and A. G. Cullis, J. Cryst. Growth **73**, 622 (1985).
[6] R. C. Anderson, R. S. Muller, and C. W. Tobias, J. Electrochem. Soc. **138**, 3450 (1991).
[7] N. Koshida, Y. Kiuchi, and S. Yosimura, in *Proceedings of the 10th Symposium on Photoelectronic Image Devices, London, 1991*, edited by B. Morgan (Institute of Physics, Bristol, 1992), p. 377.
[8] M. Ben-Chorin, F. Möller, and F. Koch, Phys. Rev. B **49**, 2981 (1994).
[9] R. L. Smith and S. D. Collins, J. Appl. Phys. **7**, R1 (1992).
[10] P. Goudeau, A. Naudon, G. Bomchil, and R. Herino, J. Appl. Phys. **66**, 625 (1989).
[11] V. Vezin, P. Goudeau, A. Naudon, A. Halimaoui, and G. Bomchil, Appl. Phys. Lett. **60**, 2625 (1992).
[12] B. J. Heuser, S. Spooner, C. J. Glinka, D. L. Gilliam, N. A. Winslow, and M. S. Boley, in *Microcrystalline Semiconductors: Materials Science & Devices*, edited by P. M. Fauchet, C. C. Tsai, L. T. Canham, I. Shimizu, and Y. Aovagi, MRS Symposia Proceedings No. 283 (Materials Research Society, Pittsburgh, 1993), p. 209.
[13] N. F. Mott and E. A. Davis, *Electronic Processes in Non-Crystalline Materials*, 2nd ed. (Clarendon Press, Oxford, 1979).
[14] H. Böttger and V. V. Bryksin, *Hopping Conduction in Solids* (Akademie-Verlag, Berlin, 1985).
[15] A. K. Jonscher, Nature **267**, 673 (1979); *Dielectric Relaxation in Solids* (Chelsea, London, 1983).
[16] A. R. Long, Adv. Phys. **31**, 553 (1982).
[17] We use the notation $\sigma(\omega) = \sigma'(\omega) + i\sigma''(\omega)$ for the complex dynamic conductivity.
[18] J. R. Macdonald, *Impedance Spectroscopy* (Wiley, New York, 1987).
[19] D. A. G. Bruggeman, Ann. Phys. (Leipzig) **24**, 636 (1935).
[20] D. J. Bergman, Ann. Phys. (N.Y.) **138**, 78 (1981).
[21] W. Theiss and P. Grosse, in *Microcrystalline Semiconductors: Materials Science & Devices* (Ref. 12), p. 215.
[22] K. L. Ngai, Comm. Solid State Phys. **9**, 127 (1979).
[23] J. P. Bouchaud and A. Georges, Phys. Rep. **195**, 127 (1990).
[24] W. Schirmacher, Ber. Bunsenges. Phys. Chem. **95**, 368 (1991).
[25] M. Pollak and T. H. Geballe, Phys. Rev. **122**, 1742 (1961); **6**, 1742 (1961).
[26] J. P. Clerc, G. Giraud, M. M. Laugier, and J. M. Luck, Adv. Phys. **39**, 191 (1990).
[27] A. R. Long, in *Hopping Transport in Solids*, edited by M. Pollak and B. I. Shklovski (North-Holland, Amsterdam, 1991), p. 207.
[28] R. A. Street, G. Davies, and A. D. Yoffe, J. Non-Cryst. Solids **5**, 276 (1971).
[29] M. Ben-Chorin, F. Möller, and F. Koch, in *Light Emission from Silicon*, edited by J.-C. Vial, L. T. Canham, and W. Lang, European Materials Research Society Symp. Proc. Vol. 43 (North-Holland, Amsterdam, 1994) [reprinted from J. Lumin. **57**, 159 (1993)].
[30] *Physics of Group IV Elements and III-V Compounds*, edited by O. Madelung, Landolt-Börnstein, New Series Group III, Vol. 17, Pt. a (Springer-Verlag, Heidelberg, 1982).
[31] J. Kočka and J. Krištofic, Phys. Status Solidi A **45**, 559 (1978).
[32] W. Schirmacher, Solid State Commun. **39**, 893 (1981).
[33] S. Summerfield, Philos. Mag. B **52**, 9 (1985).
[34] J. Dyre, Phys. Rev. B **47**, 9128 (1993).
[35] For noninteracting carriers in the case of Boltzmann statistics, we have $\partial n/\partial\mu = n/k_B T$, and for Fermi statistics $\partial n/\partial\mu = N(E_F)$, where $N(E_F)$ is the density of states at the Fermi level.
[36] J. P. Hansen and I. R. McDonald, *Theory of Simple Liquids*, 2nd ed. (Academic Press, London, 1986).
[37] S. Alexander and R. Orbach, J. Phys. **43**, L625 (1982).
[38] T. Nakayama, K. Yakubo, and R. L. Orbach, Rev. Mod. Phys. **66**, 381 (1994).
[39] B. B. Mandelbrot, *The Fractal Geometry of Nature* (Freeman, New York, 1977).
[40] D. Stauffer, *Introduction to Percolation Theory* (Taylor & Francis, London, 1985).
[41] Y. Gefen, A. Aharony, and S. Alexander, Phys. Rev. Lett. **50**, 77 (1983)

[42] The analysis of Gefen *et al.* (Ref. 41), which is based on the random walk concept adopted in the present paper, has been criticized by A. Coniglio, M. Daoud, and H. J. Herrmann, J. Phys. A. **22**, 4189 (1989), on the basis of an equivalent network analysis. However, Coniglio *et al.* did not utilize the equivalent network for the electrochemical potential [which is the correct procedure (Ref. 14)], but that for the electrical potential only. If the correct network is utilized, the results of Gefen *et al.* are reproduced [W. Schirmacher, J. Phys. A **27**, L727 (1994)].

[43] In the notation of percolation theory (Refs. 38 and 40) $\tilde{\mu} = \mu - \beta$, where μ is the conductivity exponent and β the exponent which belongs to the probability for a site to be on the infinite cluster.

[44] Since in PS we do not have evidence for variable-range hopping (Ref. 13), we ignore the fluctuations of ν_0 due to the hopping distances r_{ij}.

[45] S. Kirkpatrick, Rev. Mod. Phys. **45**, 574 (1973).

[46] R. J. Elliott, J. A. Krumhansl, and P. L. Leath, Rev. Mod. Phys. **46**, 465 (1974).

[47] C. R. Gochanour, H. Ch. Andersen, and D. M. Fayer, J. Chem. Phys. **70**, 4254 (1979).

[48] B. Movaghar, B. Pohlmann, and W. Schirmacher, Solid State Commun. **34**, 451 (1980).

[49] B. Movaghar, B. Pohlmann, and G. Sauer, Phys. Status Solidi B **97**, 553 (1980).

[50] B. Movaghar and W. Schirmacher, J. Phys. C **14**, 859 (1980).

[51] S. Summerfield and P. N. Butcher, J. Phys. C **15**, 7003 (1982).

[52] W. Schirmacher, Solid State Ion. **28-30**, 129 (1988).

[53] W. Schirmacher and M. Wagener, in *Festkörperprobleme /Advances in Solid State Physics*, edited by U. Rössler (Vieweg, Braunschweig, 1991), Vol. 31, p. 39.

[54] S. Summerfield, Solid State Commun. **39**, 401 (1981).

[55] I. Webman, Phys. Rev. Lett. **47**, 1496 (1981).

[56] T. Odagaki and M. Lax, Phys. Rev. B **24**, 5284 (1981).

[57] E. N. Economou, *Green's Functions in Quantum Physics*, 2nd ed. (Springer-Verlag, Heidelberg, 1990).

[58] The final saturation of $\sigma'(\omega) \to \langle W_{ij} \rangle$ is only observed in computer simulations but not in experiments because in the relevant frequency regime ($\approx 10^{12}$ Hz) molecular and atomic polarization phenomena become important.

[59] J. H. Kaufman, C. K. Baker, A. I. Nazzal, M. Flickner, and O. R. Melroy, Phys. Rev. Lett. **56**, 1932 (1986).

[60] D. W. Schaefer, B. J. Olivier, C. S. Ashley, D. Richter, B. Farago, B. Frick, L. Hrubesh, M. J. van Bommel, and S. Krueger, J. Noncryst. Sol. **145**, 105 (1992).

[61] A. L. Efros and B. I. Shklovskii, in *Electron-Electron Interactions in Disordered Systems*, edited by A. L. Efros and M. Pollak (North-Holland, Amsterdam, 1985).